A spike of CO_2 in the atmosphere at glacial-interglacial boundaries induced by rapid deposition of manganese in the oceans

By A. MANGINI and A. EISENHAUER, *Heidelberg Academy of Sciences, Im Neuenheimer Feld 366, D-6900 Heidelberg, Germany*, and P. WALTER, *Alfred Wegener Institut, Bremerhaven, c/o Institut für Umweltphysik der Universität Heidelberg, Im Neuenheimer Feld 366, D-6900 Heidelberg, Germany*

ABSTRACT

The model presented here provides an explanation of the rapid response of atmospheric CO_2 to increasing solar insolation. In the glacial ocean, during periods of slow, deep water renewal, when less oxygen is supplied to the deep ocean and into sediments, manganese oxide in the sediments is reduced and forms soluble $MnCO_3$ and stays in the water column. The dissolved Mn-carbonate should then reach a concentration of $\geqslant 10$ μMol/liter, approximately 5,000 to 10^4 times larger than it is at present. This is the mode prevailing until deep water formation at high latitudes starts again. As soon as the balance between oxygen and organic matter becomes oxidizing once more, the deposition of MnO_2 recommences. Oxidation of dissolved $Mn^{2+}CO_3$ to $Mn^{4+}O_2$ which is a spike of acidity to the ocean, rapidly lowers the CO_3^{--} concentration in the water column and enhances release of CO_2 to the atmosphere, producing the observed events of CO_2 increase at the transitions from glacials to interglacials. The surprising conclusion is that the oceanic (redox-) cycle of a minor element may have had a major impact on Earth's climate.

1. Introduction

It is widely accepted that there is a relationship between ice volume and the summer insolation in the northern hemisphere. The Earth's glacial cycles are driven by cyclic changes in the Earth's orbital elements. This conclusion is based on the strong coherence between the approximately 20,000 and 40,000 yearly spectral components of ice volume and insolation (Milankovitch-curve) records. These frequencies are determined by the variation of the obliquity of the Earth's axis and by its position relative to the Earth's orbit around the sun. The degree of summer insolation on the Earth's northern Hemisphere is believed to be relevant to climate because the North Atlantic is the region where cold saline water is being formed. Present-day deep-water circulation is driven by salt build-up due to net evaporation. In contrast, in the North Pacific, precipitation exceeds evaporation. Thus, deep water transfers a surplus of salt from the North Atlantic to the North Pacific. This surface water also delivers oxygen to the deep ocean. In contrast, upwelling deep water transfers nutrients from the deep ocean to the surface water. Today, the time of renewal of deep water is in the order of 1,000 years.

It is also evident that there is a link between temperature and the CO_2 concentration in the atmosphere. Recent work on ice cores from Antarctica has proven that there is a remarkable correlation between the temperature and the atmospheric CO_2 concentration, as revealed by gas bubbles trapped in the ice which are an archive of the composition of the atmosphere in the past. The profiles (measured on the ice cores) show that the maxima of the CO_2 concentration correlate with maxima of deuterium in the ice (Barnola et al., 1987; Jouzel et al., 1987). Higher deuterium concentrations in the ice are an indicator of warmer climates as they reflect the lower deuterium concentration in the oceans during warmer climates. The climatic

warming from the glacial stages 6 to the interglacial stage 5 (called the Eemian: the penultimate interglacial period corresponding to climatic stage 5e, from about 120,000 to 130,000 years B.P.) and from the last glacial stage 2 to the Holocene (the youngest geologic period that began about 12,000 years before the present), are characterized by rapid increase of the atmospheric CO_2 concentration from 180–200 ppmv to 260–290 ppmv. From about 120,000 years to 20,000 years B.P., the temperature and the CO_2 concentration in the atmosphere then decreased slowly. This downward trend was superimposed by variations of the CO_2 concentration of about 20 ppmv. The rapid increase of the CO_2 coincides with the increase of deuterium in the ice, at least within the time-resolution of the data. However, there is an apparent lag between the decrease of the temperature and CO_2 in the period from the Eemian (Stage 5) to the last ice-age.

Furthermore, it is generally accepted that the ocean, bearing the largest resevoir of CO_2, controls the CO_2 concentration in the atmosphere and its variations with time. Several models of ocean circulation have been suggested as an explanation of the change in atmospheric CO_2 concentrations from glacial to interglacials. These models have shown that the pCO_2 in the atmosphere, O_2 in the deep-sea, δC-13 and distribution of nutrients, are all tied together (Ennever and McElroy, 1984; Toggweiler and Sarmiento, 1984). Broecker and Peng (1987) have recently summarized these models in four different scenarios, which call upon a greater biological depletion of the CO_2 content of the ocean's surface water during glacial times than during interglacial times. They called these different scenarios: (i) "nutrient inventory scenario", (ii) "Redfield ratio scenario", (iii) "nutrient residence time scenario" and (iv) "ventilation rate scenario". These scenarios have one thing in common, as they show that if the currently relatively high nutrient content in high latitude surface waters was reduced by more efficient biological removal during glacial time, the CO_2 of all surface waters and the CO_2 content of the atmosphere would be correspondingly lower. The larger flux of carbon (incorporated in organic matter) into the deep ocean leads to a larger CO_2 flux to the deep ocean, because a larger amount of organic matter is remineralized in the water column, and to a shallowing of the CCD. Summarizing, these four scenarios predict lower pCO_2 in surface waters together with lower oxygen contents in the deep ocean, and more negative δC-13 values during glacial times, when the production of deep water in the North Atlantic is slowed. A slower ocean circulation transfers less oxygen into the deep ocean. Together with the increase in biological productivity, they lower the O_2 level. The slower renewal rate of deep water also leads to lower C-13 in the deep water which receives a stronger imprint from organic matter which is being oxidized at the ocean bottom (which is depleted of C-13).

There are several indications suggesting that these assumptions are correct. The Boyle and Keigwin (1982) Cd/Ca ratios in the carbonate produced by microfauna living at the bottom of the ocean (benthic foraminifera) strongly suggest a slowing of deep-water production in the North Atlantic during glacials. Negative δC-13 values in benthic foraminifera in stage 6 provide further evidence of less deep ocean ventilation during glacials (Duplessy and Shackleton, 1985). Carbon isotope data in core V19-30 also confirmed a lower CO_2 concentration in the glacial atmosphere (Shackleton et al., 1983).

An alternative recent model by Boyle (1988), which seems a more realistic approximation, explains the decrease of pCO_2 during glacials assuming a scenario where intermediate glacial ocean is depleted of CO_2 and nutrients. In contrast, the deep ocean is enriched in CO_2 and nutrients whereas the deep water O_2 concentration is approximately half the concentration during interglacials.

These models leave no doubt that the pCO_2 in the atmosphere is driven by the state of circulation of the ocean. However, the finding that for the abrupt transition from glacial to interglacial at about 130,000 years ago, no lag exists between the increase of CO_2 in the atmosphere (as recorded in the trapped air bubbles) and the temperature change (as recorded by stable isotopes Deuterium and O-18), creates a serious problem for any nutrient-based scenario. This contradiction relies on the fact that at the transition from glacial to interglacial, the nutrient scenarios all produce changes of the CO_3^{--} concentration in the ocean and that the carbonate system in the ocean requires at least several thousands of years to attain the equilibrium state. A drop of the CO_2 flux

into the ocean at the transition from glacial to interglacial due to a reduction of biological productivity, causes a surplus of CO_3^{--} that has to be removed by sedimentation of the carbonate. The lowering of this surplus of CO_3^{--} in the ocean (corresponding to re-equilibration) is accomplished via sedimentation of $CaCO_3$ (Broecker and Peng, 1987). This process requires at least 6,000 years. Therefore, one would expect the atmospheric CO_2 concentration to lag behind temperature at least for several thousands of years, until the surplus of $CaCO_3$ has been sedimented.

Despite a general consensus being attained on the basic processes driving the CO_2 concentration in the atmosphere, the cause for the rapid response of CO_2 in the atmosphere to the insolation curve at the beginning of interglacials is not yet understood.

We will present here a simple model which by deposition of manganese at the beginning of interglacials produces a significant and fast release of CO_2 to the atmosphere, solving the apparent contradiction in earlier scenarios. Our model is based on two assumptions: (i) a glacial ocean allowing build-up of Mn^{2+} in the water column and (ii) the precipitation of Mn and the formation of Mn-rich layers at the beginning of interglacials. These assumptions are supported by our data on Mn-crusts and from profiles of Mn in deep-sea sediments.

2. Release of Mn from the sediments

Several experiments on aquatic systems suggest that it is the supply of oxygen to the sediments (controlled by the diffusion through the diffusive boundary layer) that determines when Mn is being released to the water column. Apparently, when the redoxcline in the sediments (the depth level at which all of O_2 is used up for oxidation of organic matter) lies close to the water sediment interface, high concentrations of dissolved Mn occur, and diffusive loss of Mn to the water column is possible even at significant O_2 concentration levels in the water column. The slow velocity for the oxidation of Mn^{2+} to MnO_2, could explain the fact that significant amounts of Mn^{2+} are observed in oxygenated water. As shown in laboratory experiments, the oxidation rates of Mn predict a

residence time in the water column of the order of hundreds of years in the absence of particulate material, weeks to months in the presence of iron oxides, and a few days with bacterial catalysis (Emerson et al., 1982).

In Lake Constance, for example, O_2 levels in the water column never drop below 62 μMol/l (2 mg/l), even during periods of the summer stratification. In this lake, release of manganese to the water column was shown to start at an O_2 concentration of about 125 μMol/l (4 mg/l), by direct measurement of Mn and O_2 in the water column, as well as in laboratory experiments with lake sediments in regulated chambers (Ostendorp and Frevert, 1979). Bell jar experiments performed in the Kiel Bight (a fine muddy sand with $C_{org} \approx 0.8\%$) by Balzer (1982) showed release of Mn immediately after enclosure of the water mass. The Mn concentration rose at O_2 concentrations exceeding 260 μMol/l (6 ml/l) and without a decrease of the E_H. Benthic flux chamber experiments in a Swedish fjord by Sundby et al. (1986), corroborate Balzer's observation. Hall et al. (1989), give a threshold of 6 mMol m^{-2} day^{-1} (corresponding to 10^{-5} μMol cm^{-2} s^{-1}) for the uptake flux of O_2 into the sediments, at which transition from linear to exponential O_2 uptake occurs. This threshold (at about 100 μMol/l) marks the beginning of release of Mn^{2+} from the sediments. This flux corresponds to a mass transfer velocity across the diffusive boundary layer of 10^{-4} cm/s ($\beta =$ 10^{-5} μMol/cm^2 s divided 100 μMol/l). Applying the relationship between mass transfer and deep ocean velocity derived in Boudreau and Scott (1978), this mass transfer velocity corresponds to a deep water velocity of <2 cm/s, applying the molecular diffusion coefficient of O_2 of 15.7·10^{-6} cm^{-2} s^{-1} (Hall et al., 1989). Present-day supply of Mn^{2+} from the sediments is negligible because at an average velocity of deep water in the range of 4 cm/s, the flux of O_2 into the sediments is approximately 10 Mol m^{-2} yr^{-1}. This is an amount comparable to the flux of the biologically-produced organic matter in the surface of the ocean, and therefore it is large enough to account for oxidation of all organic matter supplied to the sediments. This conclusion corroborates observations suggesting that in the interglacial ocean having a well-oxigenated bottom water, the redoxcline lies so deep in the

sediment column that Mn^{2+} migration into the water column is not possible (Froelich et al., 1979).

However, in the glacial deep ocean with significantly lower O_2 concentration levels at about 100 μMol/l (Boyle, 1988), a higher C_{org} content in the sediments (Emerson and Hedges, 1988), and overall slower deep water circulation, conditions for release of Mn to the water column could be possible. The flux of O_2 into the sediments at a deep water velocity of 0.5 cm/s, estimated to be as low as 0.32 Mol m^{-2} yr^{-1}, comes close to the flux of organic matter supplied to the sediment surface (some percentage of the production flux).

We assume that in the glacial ocean, Mn-oxide is supplied from the sediments, which provide a huge reservoir of manganese. Holland (1984) estimated that if the entire ocean floor was suboxic, the production rate of $Mn(2+)$ would be 20×10^{12} g/yr ($=0.1$ μMol cm^{-2} yr^{-1}). The time required to transfer 2.5 mMol $Mn(2+)$ to a water column of 2,500 m (with a concentration of 10 μMol/liter) would be approximately 25 kyr. This is possibly an upper limit. The flux of Mn released into the water column in the bell jar experiments ranges between 13 and 41 μMol cm^{-2} yr^{-1} (Balzer, 1982). In anoxic sediments, fluxes as high as 251 μMol cm^{-2} yr^{-1} have been reported (Eaton, 1979). Thus the time constant to transfer 2,500 μMol cm^{-2} to the water column in the glacial ocean could have been in the range of 100 years or even shorter if parts of the ocean bottom were anoxic. Other important sources of Mn could be hydrothermalism and river water, if Mn is not precipitated as the rivers enter the oceans.

Our estimate of the time constant for supplying the Mn is of the same order of magnitude as the residence time of Mn in the interglacial ocean estimated at 60–100 years, suggesting that build-up of Mn can easily be achieved just from Mn-fluxes from sediments.

The solubility of $MnCO_3$ in the water column at $p_H = 8$ (1 atm and 25°C) is approximately 10^{-5} Mol/liter (Stumm und Morgan, 1970). This agrees with the observed maximum of the Mn concentration of $0.8 \cdot 10^{-5}$ Mol/liter in the Black Sea (Holland, 1984). However, applying corrections for the temperature and for pressure in deep sea sediments (1.6°C and 310 bars), the solubility of $MnCO_3$ was estimated to be at least 10^{-4} Mol/liter (Klinkhammer and Bender, 1980).

The concentration of Mn^{2+} observed in pore waters of pelagic sediments was as high as 100 μMol/kg (or 5500 μg/kg).
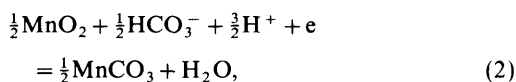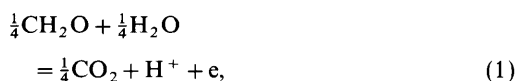
3. The behaviour of Mn in the Ocean

Mn undergoing redox processes in the ocean behaves in a peculiar way. At present, the Mn content in the water column in the open ocean is extremely low (0.05–0.1 ppb or 1–2 nMol/liter) (Landing and Bruland, 1979, Klinkhammer and Bender, 1980). The highest concentrations below the surface layer have been observed in the oxygen minimum layer. Horizontal advection along this layer probably supplies Mn to the open ocean from near-shore areas where Mn is being remobilized from reducing sediments (at $E_H < 0$). However, the major source of Mn in the ocean is hydrothermalism (Mangini et al., 1990). In the open ocean, under present-day conditions ($p_H = 8.1$, $pO_2 = 0.2$, $E_H = 0.4 - 0.5$ V), Mn is oxidized to MnO_2, which is then sedimented to the ocean bottom. The present-day flux of Mn to pelagic sediments can be estimated at some mg cm^{-2}/1000 yr (corresponding to 18 μMol cm^{-2}/1000 yr). The behaviour of Mn is visualized on the $p_\varepsilon - p_H$ diagram in (Fig. 10–6 in Stumm and Morgan, 1970). The half-cell reaction of the redox process has a $p_\varepsilon^0 = 8.5$ corresponding to $E_H^0 = 0.5$ V (at 25°C). This means that $Mn(4+)$ will be reduced to $Mn(2+)$ at E_H values < 0.5 V, but larger than 0, i.e., before the deep water system becomes anoxic.
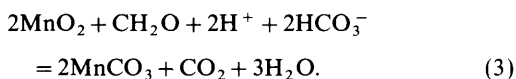
The E_H of the ocean of 0.4–0.5 V is nearly independent of the O_2 concentration in the water column. It is assumed that the oxidation potential of the ocean is controlled by the H_2O_2-O_2 couple, i.e., oxidation by oxygen has to go through a rate-controlling hydrogen peroxide step (Garrels and Christ, 1965; Sato, 1960). Sato explains the mechanism of oxidation potential control by oxygen by assuming that until the potential of the H_2O_2-O_2 couple is reached, ions in solution are quickly oxidized by hydrogen peroxide produced from oxygen oxidation. When the oxidation potential of the solution exceeds that of the H_2O_2-O_2 couple (when, e.g., the supply of reducing agents into the water column is higher than at present), Mn-oxide may act as a catalyst for oxidation of the peroxide back to oxygen. This means that oxygen

is no longer available for oxidation, though it may be abundant in the solution. To lower the E_H in the water column to values of < 0.5 V and thus to produce Mn^{2+}, requires a strong reductant. We assume that during glacial periods, when not enough oxygen is supplied to the deep water, this reductant is organic matter that was not oxidized by O_2.

The half-cell equations for the oxidation of organic matter (where $1/n$ $(CH_2O)_n$ is simplified to CH_2O) and for the reduction of Mn-oxide in the sediments (Stumm and Morgan, 1970) are:
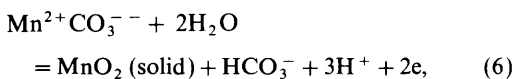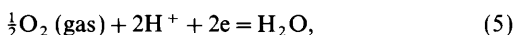
$$\tfrac{1}{4}CH_2O + \tfrac{1}{4}H_2O$$
$$= \tfrac{1}{4}CO_2 + H^+ + e, \tag{1}$$
$$\tfrac{1}{2}MnO_2 + \tfrac{1}{2}HCO_3^- + \tfrac{3}{2}H^+ + e$$
$$= \tfrac{1}{2}MnCO_3 + H_2O, \tag{2}$$

yielding:

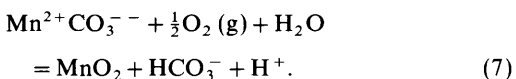$$2MnO_2 + CH_2O + 2H^+ + 2HCO_3^-$$
$$= 2MnCO_3 + CO_2 + 3H_2O. \tag{3}$$

4. The impact of Mn on the CO₂ system

Deposition of MnO_2 probably recommences in the North Atlantic when the value of net evaporation increases and thus when deep water is being formed at a higher rate and more oxygen is supplied to the deep sea. The concentration of Mn in the water column then rapidly drops to present-day values. The half-cell equations for oxidation of Mn are:

$$\tfrac{1}{2}O_2 \, (gas) + 2H^+ + 2e = H_2O, \tag{5}$$
$$Mn^{2+}CO_3^{--} + 2H_2O$$
$$= MnO_2 \, (solid) + HCO_3^- + 3H^+ + 2e, \tag{6}$$

yielding:

$$Mn^{2+}CO_3^{--} + \tfrac{1}{2}O_2 \, (g) + H_2O$$
$$= MnO_2 + HCO_3^- + H^+. \tag{7}$$

This reaction converts 10 μMol of CO_3^{--} into HCO_3^- and delivers additionally 10 μMol H^+, assuming the concentration of $MnCO_3$ in ocean water to be 10 μMol/liter. Thus, oxidation of

manganese carbonate, by which the acidity of the ocean is suddenly raised (via addition of H^+ ions or subtraction of OH^-), significantly lowers the $[CO_3^{--}]$ concentration in the water to produce $[HCO_3^-]$. Following Broecker and Peng's (1982) notation

$$pCO_2 \, (air) = \frac{const. \, [HCO_3^-]^2}{[CO_3^{--}].} \tag{8}$$

Present-day concentrations in the oceans are:
$[CO_3^{--}]$: 90 μMol/liter and
$[HCO_3^-]$: 2070 μMol/liter.

Eq. (8) shows that lowering of dissolved $[CO_3^{--}]$ correspondingly changes the pCO_2 in the atmosphere. Addition of 20 μMol of H^+ produced in approximately $\tfrac{2}{3}$ of the water column will lower the $[CO_3^{--}]$ concentration (presently at 90 μMol) by some 19% and consequently raise the pCO_2 in the atmosphere by the same proportion, i.e., from 190 ppmv to 226 ppmv, which is close to half the observed change between glacials and interglacials.

The process of oxidation of Mn occurs in the water column and its effect on the CO_3^{--} concentration is immediate, as it counteracts the rise of CO_3^{--} induced by a reduced biological productivity. Oxidation of Mn will occur on a time scale similar to that of the renewal time of deep water in the ocean. This time scale is much shorter than the time scale evaluated in thise scenarios relating the CO_2 increase in interglacials to less bioproductivity, where excess of CO_3^{--} will be compensated by sedimentation of calcium carbonate, a process that requires at least 3,000 to 6,000 years (Broecker and Peng, 1987, Boyle, 1983). This means that the ocean will release an amount of CO_2 as a fast response to the initial triggering (increase of solar summer insolation and of temperature) and magnify the climatic response to the Milankovitch insolation curve without any significant delay.

Thus, this process gives an explanation for the synchronous response of atmospheric CO_2 and temperature, as observed in the record from ice cores. It also explains why there is no evidence of significant change in the carbonate compensation depth in the ocean at the end of a glacial.

The standing crop expected in sediments from rapid deposition of 10 μMol/liter of manganese oxide would be 137 mg/cm². Finally, in a rather

unrealistic scenario where the "biological pump" is negligible and oxidation of Mn is assumed to be the only mechanism raising the atmospheric CO_2 at the end of a glacial, the concentration of dissolved $MnCO_3$ in the water column would have to be at least 26 μMol/liter. The standing crop in the sediments would then amount to 286 mg/cm^2. Future studies of Mn distribution in sediment cores will help to better assess the impact of Mn on the CO_2 system.

5. Preliminary testing of the model

We have checked whether the assumptions of build up of $MnCO_3$ in a less ventilated ocean are valid and whether the conclusions derived here are correct, by examining Mn-cursts and pelagic sediments. In Mn-crusts, we observed slower growth rates or growth standstill during glacials, when no $MnCO_2$ is deposited on the ocean bottom. In marine sediments, we observed spikes of Mn at the beginning of interglacials.

5.1. Mn-crusts

In two Mn-crusts (VA-13-2 from 146°W, 9°25'S, water depth: 4830 m, and 72DK9 170°35'W, 20°13'N, water depth: 1550 m), the climatic cycles during the past 300 kyr were determined at the required resolution with Th-230. These two samples were analyzed in our lab with a special technique that attained a depth resolution of 20 μm/depth interval, corresponding to 5–7 kyr. Here we will briefly present the results (from Eisenhauer (1986) and Balmer (1988)), which will be discussed in greater detail elsewhere.

The high resolution Th-230 profile in VA 13-2 shows three sections with an average growth rate of 6.6 to 5.8 mm/my, and nonconformities of the Th-230 concentration at 0.89 mm and at 1.29 mm depth. These nonconformities were attributed to periods of growth standstill between 130 and 180 kyr B.P. and between 240 and 280 kyr B.P., of duration 40 ± 8 kyr and 28 ± 8 kyr, respectively.

The high resolution profile in the ferromanganese crust 72DK9 reveals sections of minimum and maximum concentration of Th-230, which could be attributed to variable dilution of Th-230 (produced at a constant rate in the water column) with MnO_2. Applying a "constant Th-230 flux model", we convert the Th-230 concentration into

growth rates. Fig. 1 shows growth rates in each sample against the age scale (Figs. 1a, b show sections of faster growth (up to 9 mm/Myr) and sections of slower growth). The ages for the "fast" sections correspond to interglacials; slower growth rates correspond to glacial stages 6, 8 and 3.

5.2. Sediments from high latitudes

Core 23055 was sampled in the Norwegian Sea at a water depth of 2311 m. In this core, both Mn and O-18 Profiles are reported (Fig. 2a) (Henrich et al., 1989). A prominent peak of Mn (corre-
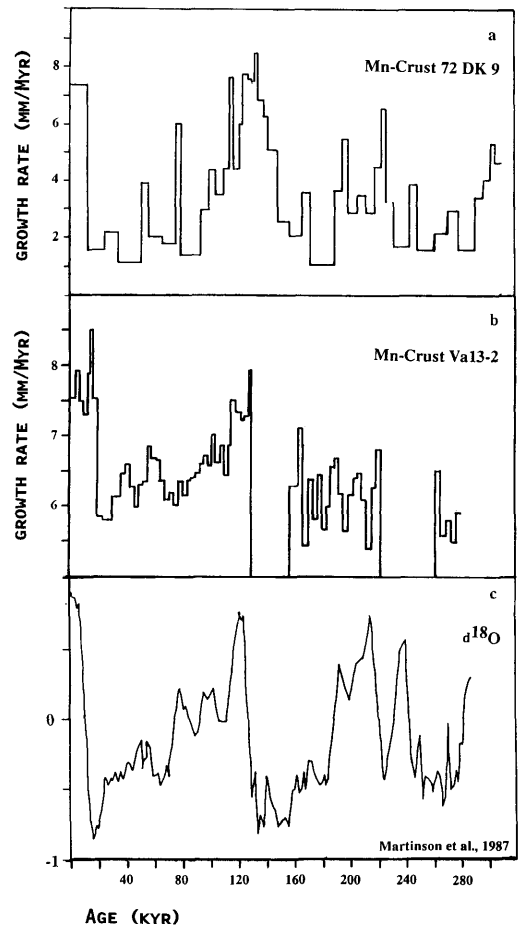

Fig. 1. Growth rates of Mn-crusts 72 DK 9 (a) and VA 13-2 (b) derived by applying a constant flux model on the Th-230 depth profile, against age (from Eisenhauer et al., 1990). (c) Generalized δO-18 chronostratigraphy after Martinson et al. (1987).

sponding to about 50 mg/cm^2) is observed at the glacial-interglacial boundary between stages 5 and 6. Data at boundary 2 to 1 are not available due to missing core top.

Core M23235-2 from the Fram Strait (78°51.5' N, 1°18.59' E) was taken at 2456 m water depth. In this core covering the last 280,000 years, we obtained high-resolution stratigraphy from the measurement of high-resolution Th-230 and Be-10 depth profiles at a resolution comparable to the O-18 method (Eisenhauer et al., 1990). The average sediment accumulation rate is approximately 3 cm/1000 years. The flux of Mn in the core was determined as the product of Mn-concentration, partial sedimentation rate and in situ density. As shown in Fig. 2c, peaks of Mn precede the boundaries between climatic stages 1/2, 3/4 and 5/6 that are calibrated at 12,000, 59,000 and 130,000 years. Further peaks are observed at 100,000 years B.P., 242,000 years, 250,000 years and at 275,000 years B.P. The standing crop of Mn in excess of the base-line in these peaks is approximately 42.5 mg/cm^2 (at 12,000 years),

45 mg/cm^2 (at 60,000 years) and 40 mg/cm^2 (at 140,000 years).

Core 1170-3 was sampled in the Weddell Sea in an area south of the South Orkney Islands, at a water depth of 4,000 m (Walter et al., 1989). The average accumulation rate amounts to 3 cm/kyr, determined from Th-230 stratigraphy. Based on Th-230 (as well as on the profile of the concentration of Ca and Ba), stage 5e is dated at 450 cm. The profile of Mn (Fig. 2d) displays a base level of about 0.05% and prominent peaks at 150 cm (0.7%), 450 cm (0.3%) and 30 cm (0.3%). In these peaks, the standing crops of Mn in excess of the base level amount to between 60 and 130 mg/cm^2.

5.3. Sediments from the Central Pacific

Spikes of manganese down core have been observed in sediment cores from the Central Pacific (Finney et al., 1988; Berger et al., 1983). Berger et al. report that over large areas of the tropical Pacific, calcareous sediments show one or more dark-coloured manganese rich layers within
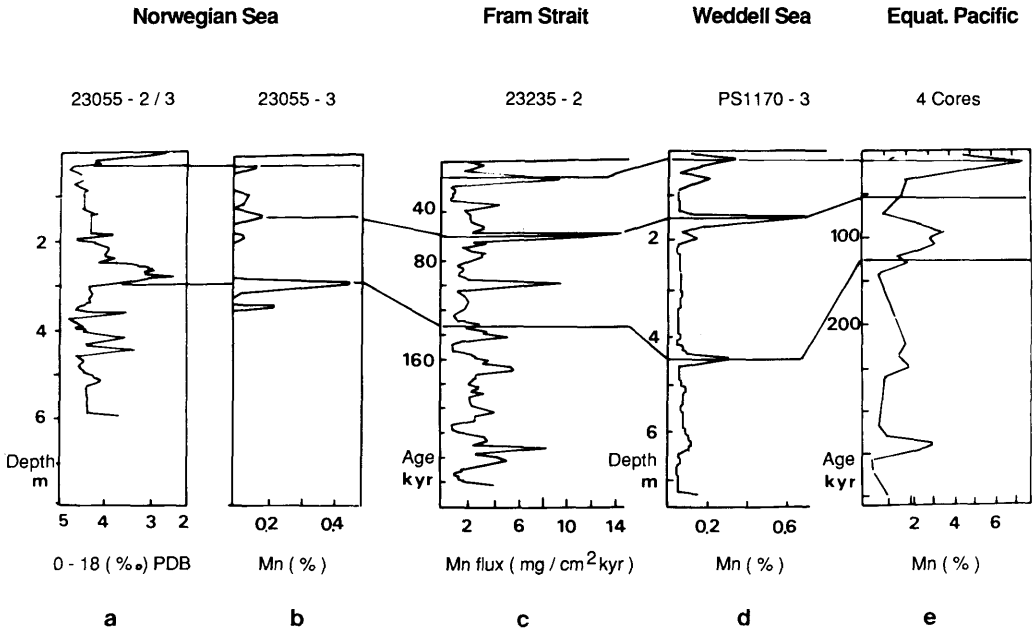

Fig. 2. (a) and (b). Profiles of O-18 and Mn in core 23055-3 from the Norwegian Sea. (c) Profile of the Mn flux together with the stratigraphy based on the Th-230 and Be-10 profiles in core 23235-2 from the Framstrait. (d) Profile of Mn in core 1170-3 from the Weddell Sea. (e) Profile of the manganese concentration in cores Vulcan I-49Gc, 38GC, 70GC and 63GC (from Finney et al. (1988)).

the uppermost 40 cm of the record. The lower peak in box core PLDS 72 consists of an increase of the Mn concentration from a base-line value of 0.4 % to 1.3 %. This layer is centered on the glacial-Holocene boundary. The standing crop of "excess" Mn in the lower layer amounts to approximately 42 mg/cm^2. Finney et al. (1988) report that gravity cores recovered from the Mn-nodule Project Site H show marked down core variations in the abundance of Mn together with organic carbon, opal and other components (Fig. 2e). The Mn-peaks in these cores correspond to interglacial stages 5, 7 and 9. In the core 49GC, the standing crop of Mn may be evaluated at 400 mg/cm^2 (in the layer corresponding to the glacial-holocene boundary), at about 350 mg/cm^2 (in stage 5), at 171 mg/cm^2 (in stage 7) and at 332 mg/cm^2 (in stage 9), assuming a base-line level of 1 % and a density of 0.7 g/cm^3. Maximum standing crop levels at 530 mg/cm^2 are attained in stage 5 of their core 70GC.

6. Conclusions

The facts that: (1) Mn-peaks in the sediments are at the glacial-interglacial boundaries; (2) they are time-synchronous; (3) they have the expected magnitude (40–530 mg/cm^2); (4) they did not rapidly redissolve (probably because of a larger grain-size), together with; (5) the data from the Mn-encrustations; provide strong evidence for the loading of the water column with Mn^{2+} during glacials and suggest that the Mn peaks in the

sediments may have originated from a rapid precipitation on Mn from the water column.

In summary, the standing crops of Mn observed in the sediment cores are consistent with the hypothesis presented above, because they come close to (and even exceed) the value of 137 mg/cm^2 expected for the rapid deposition of 10 μMol MnO$_2$ (: 10 μMol/liter $\times$ 250 liter/cm^2 $\times$ 55 g/mol) as assumed in our model.

One of the major unknowns relies on the amount of Mn sedimented with the Mn spikes at the warming event. In sediment accumulating at very low rates, these peaks might have become lost due to redissolution.

Another major unknown in our model lies in the amount of CO$_2$ that was used up in dissolution of carbonate on the ocean floor. However, the transfer time of CO$_2$ to the atmosphere was faster than the response time of the carbonate system, suggesting that the larger part of this CO$_2$ was transferred into the atmosphere. The astonishing conclusion is that the oceanic (redox-) cycle of manganese may have had a major impact on the Earth's climate.

7. Acknowledgements

REFERENCES

Barnola, J. M., Raynaud, D., Korotkevich, Y. S. and Lorius, C. 1987. Vostok Ice Core provides 160,000 years record of atmospheric CO$_2$. Nature 329, 408–414.

Balmer, W. 1988. High resolution Th-230 Dating of the Mn-crusts VA 13 − 2 from the Central Pacific. Examensarbeit, Univ. Heidelberg, 42 pp.

Balzer, W. 1982. On the distribution of iron and manganese at the sediment/water interface: thermodynamic versus kinetic control. Geochim. Cosmochim. acta 46, 1153–1161.

Berger, W. H., Finkel, R. C., Killingley and Marchig, V. 1983. Glacial-Holocene transition in deep sea sediments: manganese spike in the east equatorial Pacific. Nature 303, 231–233.

Broecker, W. S. and Peng, T.-H. 1982. Tracers in the sea. Eldigio Press, New York, 690 pp.

Broecker, W. S. and Peng, T.-H. 1987. The role of CaCO$_3$ compensation in the glacial to interglacial CO$_2$ change. Glob. Biogeochem. Cycles 1, 15–30.

Boudreau, B. P. and Scott, M. R., 1978, A model for diffusion-controlled growth of deep-sea manganese nodules, Am. J. Science 278, 903–929.

Boyle, E. A. and Keigwin, L. D. 1982. Deep circulation of the North Atlantic over the last 150,000 years; geochemical evidence. Science 218, 784–787.

Boyle, E. A. 1983. Chemical accumulation variations under the Peru current during the past 130,000 yr. J. Geophys. Res. 88, 7667–7680.

Boyle, E. A. 1988. The role of vertical chemical

fractionation in controlling late quaternary atmospheric carbon dioxide. *J. Geophys. Res. 93*, 701–714.

Duplessy, J. C. and Shackleton, N. J. 1985. Response of global deep water circulation to Earth's climate. *Nature 316*, 500–507.

Eaton, A. 1979. The impact of anoxia on Mn fluxes in the Chesapeake Bay. *Geochim. Cosmochim. Acta 43*, 429–432.

Eisenhauer, A. 1986. *High-resolution Th-230 Dating of Mn-crusts*. Examensarbeit, Univ. Heidelberg, 52 pp.

Eisenhauer, A., Mangini, A., Botz, R., Walter, P., Beer, J., Bonani, G., Suter, M., Hofmann, H. J. and Wölfli, W. 1990. High resolution Be-10 and Th-230 stratigraphy of polar core 23235-2. In: *Geological history of the Polar Ocean: Artic versus Antartic* (eds. Bleil, U., Thiede, J.). Kluwer Academic Publishers, Dordrecht, 475–487.

Emerson, S., Kalhorn, S., Jacobs, L., Tebo, B. M., Nealson, K. H. and Rosson, R. A. 1982. Environmental oxidation rate of manganese (II): bacterial catalysis. *Geochim. Cosmochim. Acta 46*, 1073–1079.

Emerson, S. and Hedges, J. I. 1988. Processes controlling the organic carbon content of open ocean sediments. *Paleoceanography 3*, 621–634.

Ennever, F. K. and McElroy, M. B. 1984. Change in atmospheric CO$_2$: factors regulating the glacial to interglacial transition. In: *The carbon cycle and atmospheric CO$_2$: Natural variation Archean to present* (eds. Sundquist, E. T. and Broecker, W. S.). Geophys. Monogr. Series, Vol. 32 Washington DC, pp. 154–162.

Finney, B. P., Lyle, M. W. and Heath, G. R. 1988. Sedimentation at manop site H (Eastern equatorial Pacific), over the past 400,000 years: climatically induced redox variations and their effects on transition metal cycling. *Paleoceanography 3*, 169–189.

Froelich, P. N., Klinkhammer, G. P., Bender, M. L., Luedke, L. A., Heath, G. R., Cullen, C., Dauphin, P., Hammond, D., Hartmann, B. and Maynard, V. 1979. Early oxidation of organic matter in pelagic sediments of the Eastern Equatorial Pacific, suboxic diagenesis. *Geochim. Cosmochim. Acta 43*, 1075–1090.

Garrels, R. M. and Christ, C. L. 1965. *Solutions, minerals and equilibria*. Harper and Row, New York, 450 pp.

Hall, P. O. J., Anderson, L. G., Rutgers van der Loeff, M. M., Sundby, B. and Westerlund, S. F. G. 1989. Oxygen uptake kinetiks in the benthic boundary layer. *Limnol. Oceanogr. 34*, 734–746.

Henrich, R., Kassens, H., Vogelsang, E. and Thiede, J. 1989. The sediment facies record of glacial/interglacial cycles: Paleoceanography and paleoclimate of the Norwegian Sea during the last 350,000 years. *Marine Geology 86*, 283–319.

Holland, H. D. 1984. *The chemical evolution of the atmosphere and oceans*. Princeton Univ. Press, 582 pp.

Jouzel, J., Lorius, C., Petit, J. R., Genthon, C., Barkov, N. I., Kotlyakov, V. M. and Petrov, V. M. 1987. Vostok ice core: a continuous isotope temperature record over the last climatic cycle (160,000 years). *Nature 329*, 403–409.

Klinkhammer, G. P. and Bender, M. L. 1980. The distribution of manganese in the Pacific Ocean. *Earth. Planet. Sci. Lett. 46*, 361–384.

Landing, W. M. and Bruland, K. W. 1980. Manganese in the North Pacific. *Earth. Planet. Sci. Lett. 49*, 45–56.

Mangini, A., Eisenhauer, A. and Walter, P. 1990. The response of manganese in the oceans to the climatic cycles in the quaternary. *Paleoceanography*, in press.

Martinson, D. G., Pisias, N. G., Hays, J. D., Imbrie, I., Moore, T. C. and Shackleton, N. J. 1987. Age dating and the orbital theory of the ice ages; Development of a high-resolution 0 to 300,000 year chronostratigraphy. *Quat. Res. 27*, 1–29.

Ostendorp, W. and Frevert, T. 1979. Untersuchungen zur Manganfreisetzung und zum Mangangehalt der Sedimentoberschicht im Bodensee. *Arch. Hydrobiol./ Suppl. 55*, 255–277.

Sato, M. 1960. Oxidation of sulfite ore bodies, 1. Geochemical environments in terms of Eh and pH. *Economic Geology 55*, 928–961.

Shackleton, N. J., Hall, M. A., Line, J. and Cang Shuxi. 1983. Carbon isotope date in core V19-30 confirm reduced CO$_2$ concentration in the ice age atmosphere. *Nature 306*, 319–322.

Stumm, W. and Morgan, J. J. 1970. *Aquatic chemistry*, Wiley-Interscience, New York, 583 pp.

Suess, E. and Müller, P. J. 1980. Productivity, sedimentation rate and sedimentary organic matter in the oceans. II. Elemental Fractionation, *Colloques internationaux du C.N.R.S., no. 293*, Paris, 17–26.

Sundby, B., Anderson, L. G., Hall, P. O. J., Iverfeldt, A., Rutgers van der Loeff, M. M. and Westerlund, S. F. G. 1986. The effect of oxygen on release and uptake of cobalt, manganese, iron and phosphate at the sediment-water interface. *Geochim. Cosmochim. Acta 50*, 1281–1288.

Toggweiler, J. R. and Sarmiento, J. L. 1984. Glacial to interglacial changes in atmospheric CO$_2$: the critical role of ocean surface water in high latitudes. In: *The carbon cycle and atmospheric CO$_2$: natural variation, Archean to present* (eds. E. T. Sundquist and W. S. Broecker). Geophys. Monogr. Series, Vol. 32 Washington DC, 163–184.

Walter, P., Eisenhauer, A. and Mangini, A. 1989. [230]Th and [10]Be chronology of sediments from the Weddell Sea, paper presented at the *Third Int. Conf. on Paleoceanography*, Cambridge, Sept. 1989. Terra abstracts, no. 1, p. 55.